SUPPLEMENTAL MATERIAL

Cis regulation within a cluster of viral microRNAs

Monika Vilimova[1,#], Maud Contrant[1,2,#], Ramy Randrianjafy[1], Philippe Dumas[3], Endrit Elbasani[4,5], Päivi Ojala[4], Sébastien Pfeffer[1,‡,*], Aurélie Fender[1,‡,*]

[1] Université de Strasbourg, Architecture et Réactivité de l'ARN, Institut de Biologie Moléculaire et Cellulaire du CNRS, 2 allée Konrad Roentgen, 67084 Strasbourg, France

[2] Present address: French Agency for Food, Environmental and Occupational Health & Safety, Laboratory of Ploufragan-Plouzané-Niort, Unit of Viral Genetics and Biosafety, Ploufragan, France

[3] Institut de Génétique et Biologie Moléculaire et Cellulaire (IGBMC), Department of Integrated structural Biology, 1 rue Laurent Fries, BP10142, F-67404 Illkirch-Graffenstaden, France

[4] Translational Cancer Medicine Research Program, P.O. Box 63 (Haartmaninkatu 8), FIN-00014 University of Helsinki, Finland

[5] Present address: Orion Corporation, Orion Pharma, Tengströminkatu 8, 20360 Turku, Finland

[#,‡]These authors contributed equally.

*To whom correspondence should be addressed: a.fender@ibmc-cnrs.unistra.fr; s.pfeffer@ibmc-cnrs.unistra.fr

SUPPLEMENTAL METHOD

Kinetic analysis

Practical problems and fitting method. There is a significant upward curvature of the low-amplitude cleavage curves around t = 0 (see for example pre-mir-K2 and pre-miR-K7 for 20130530). This was interpreted as a linearity problem of the IP response since this is only visible for the low-amplitude curves (accordingly, it is almost invisible with the Exp#1 data having higher amplitudes). Such a feature cannot be accounted for by equations (3) and (3') (see main manuscript) imposing a downward curvature around t = 0. In order to nevertheless use these equations, a simple correction was devised to mimic this lack of linearity for the lowest values of $K_i(t)/R_0$. For this, instead of using directly $Y_i = K_i(t)/R_0$ to fit the experimental curves, a modified value of Y_i was used according to the response function:

$$Y_i \rightarrow \mathcal{R}(Y_i) = \frac{(Y_i/\varepsilon)^2}{1+(Y_i/\varepsilon)^2}\, Y_i + \frac{1}{1+(Y_i/\varepsilon)^2}\, {Y_i}^2 \qquad (4)$$

with ε a small value. This response function gives $\mathcal{R}(Y_i) \approx {Y_i}^2$ for Y_i of order ϵ, which provides the upward curvature close to $Y_i = 0$, and it is transformed smoothly into $\mathcal{R}(Y_i) = Y_i$ for increasing values of Y_i above ϵ. This *ad-hoc* procedure was quite effective to improve the quality of results, particularly for the Exp#2 data. The value of ε was tuned to 0.5 % to obtain the best fit of all curves with a minimum value of the global sum of the errors on f_i and k_i^+ for both data sets. Such a low value indicates that the correction is indeed a minor one. Practically, the fit was done with the function NonlinearModelFit (with Method → "ConjugateGradient") in *Mathematica* V.11 from Wolfram Research.

Using a more stringent kinetic model of pri-miRNA cleavage. The simple model used in the study allowed us to obtain excellent fits (Figure 1 and Figure S1), but with three free parameters (f_i , k_i^+ and k_i^-) per experimental curve. In order to use a more stringent test, we imposed two restrictions for a better representation of reality. First, we imposed that the variations of the rates of cleavage by Drosha from one experiment to another one should only result from the amount of Drosha in each experiment. For this, we imposed a strict proportionality of the two sets of k_i^+. Second, we imposed that the cleaved fraction f_i of R_0 yielding the pre-miR K_i was the same for the two experiments (Figure S2). This more stringent method, therefore, involves only two adjustable parameters per curve, which represents quite a significant reduction of the degrees of freedom.

The fitting of the experimental cleavage curves with the kinetic model with three free parameters (see Material and Methods) per curve led to excellent agreement (Figure 1B and Figure S1B). Note that the slight correction for non-linearity (see Supplemental Material) was important to obtain this result. As expected, the results with a more stringent model with only two free parameters per curve were less good but mostly for the low-amplitude curves with the lowest signal-to-noise ratio (Figure S2). This indicates that the excellent agreement with three parameters was not simply the result of a meaningless numerical fit, which is in good support for the simple kinetic model in use. The numerical results are shown in Table S1.

***In vitro* pre-miRNA stability assays**

Measure of stability of *in vitro* transcribed pre-miRNAs was performed in the same conditions as the in vitro Drosha miRNA processing assays (see Materials and Methods) except that whole cell lysate was used without overexpressing Drosha and DGCR8. Briefly, 500 fmol of each of the four tested pre-miRNAs were pooled together, denatured, let to refold and incubated in total HEK293Grip cells extract for increasing times at 37°C. 1/10 of the phenol-extracted and ethanol-precipitated RNAs was used for northern blot analysis. A standard curve was generated by loading decreasing amounts (50 to 3.125 fmol) of corresponding *in vitro* transcribed pre-miRNAs.

SUPPLEMENTAL TABLES

Table S1. Sequences of oligonucleotides used in this study.

Usage	Sequence 5' to 3'	Name
RNA preparation	GAAATTAATACGACTCACTATAGAATGCGTGCTTCTGTTTGAAGG	Pri-miR-K10/12 T7 forward primer
	TTTACCGAAACCACCCAGAGGC	Pri-miR-K10/12 Reverse primer
	GAAATTAATACGACTCACTATAGATTACAGGAAACTGGGTGTAAG	Pre-miR-K1 T7 forward primer
	GGTTGCAGGAAACAGGTGCTG	Pre-miR-K1 reverse primer
	GAAATTAATACGACTCACTATAGAACTGTAGTCCGGGTCGATC	Pre-miR-K2 T7 forward primer
	CAGCTCTAGCCCTGGAAGATC	Pre-miR-K2 reverse primer
	GAAATTAATACGACTCACTATAGTCACATTCTGAGGACGGCAG	Pre-miR-K3 T7 forward primer
	TGTCACATTCTGTGACCGCGA	Pre-miR-K3 reverse primer
	GAAATTAATACGACTCACTATAGAGCTAAACCGCAGTACTCTAGGG	Pre-miR-K4 T7 forward primer
	TCAGCTAGGCCTCAGTATTCTA	Pre-miR-K4 reverse primer
	GAAATTAATACGACTCACTATAGAGGTAGTCCCTAGTGCCCTAAG	Pre-miR-K5 T7 forward primer
	CCGGCAAGTTCCAGGCATCCTA	Pre-miR-K5 reverse primer
	GAAATTAATACGACTCACTATAGCCAGCAGCACCTAATCCATCG	Pre-miR-K6 T7 forward primer
	CTCAACAGCCCGAAAACCATCA	Pre-miR-K6 reverse primer
	GAAATTAATACGACTCACTATAGAGCGCCACCGGACGGGGATTTATG	Pre-miR-K7 T7 forward primer
	AGCGCCAGCAACATGGGATCA	Pre-miR-K7 reverse primer
	GAAATTAATACGACTCACTATAGACTCCCTCACTAACGCCCCG	Pre-miR-K8 T7 forward primer
	CGTGCTCTCTCAGTCGCGCCTA	Pre-miR-K8 reverse primer

	GAAATTAATACGACTCACTATAGACCCAGCTGCGTAAACCCCG	Pre-miR-K9 T7 forward primer
	TTACGCAGCTGCGTATACCCAG	Pre-miR-K9 reverse primer
	GAAATTAATACGACTCACTATAGGTCACAGCTTAAACATTTCTAG	Pre-miR-K11 T7 forward primer
	TCGGACACAGGCTAAGCATTAA	Pre-miR-K11 reverse primer
	GAAATTAATACGACTCACTATAGGCTCGTGTTTGGGCAAAACACATC	Cut-K1 T7 forward primer
	Same as pri-miR-K10/12 reverse primer	Cut-K1 reverse primer
	Same as pri-miR-K10/12 T7 forward primer	Cut-K3 5' fragment T7 forward primer
	TAGCCCATTACAGGCATTGTAG	Cut-K3 5' fragment reverse primer
	GAAATTAATACGACTCACTATAGGCCCCTCCAGGTCCAAGCGACG	Cut-K3 3' fragment T7 forward primer
	Same as pri-miR-K10/12 reverse primer	Cut-K3 3' fragment reverse primer
Northern blot	GCTTACACCCAGTTTCCTGTAAT	Probe for miR-K1
	CAGATCGACCCGGACTACAGTT	Probe for miR-K2
	TCGCTGCCGTCCTCAGAATGTGA	Probe for miR-K3
	TCAGCTAGGCCTCAGTATTCTA	Probe for miR-K4-3p
	CCGGCAAGTTCCAGGCATCCTA	Probe for miR-K5
	CTCAACAGCCCGAAAACCATCA	Probe for miR-K6-3p
	AGCGCCAGCAACATGGGATCA	Probe for miR-K7
	CGTGCTCTCTCAGTCGCGCCTA	Probe for miR-K8
	AGCGGGGTTTACGCAGCTGGGT	Probe for miR-K9
	TCGGACACAGGCTAAGCATTAA	Probe for miR-K11
	CGCCAATATTTACGTGCTGCTA	Probe for hsa miR-16

	AACTATACAACCTACTACCTCA	Probe for hsa Let-7a
Mutagenesis	GGTGCTGCCCAGGACGGCCGGATGCGGGCGCTCGTGTTTGGGCAAAACACATCCGCTGCC	Forward primer to delete pre-miR-K1
	GGCAGCGGATGTGTTTTGCCCAAACACGAGCGCCCGCATCCGGCCGTCCTGGGCAGCACC	Reverse primer to delete pre-miR-K1
	CGCAACAGCTACAATGCCTGTAATGGGCTACCCCTCCAGGTCCAAGCGACGAACCGCCCG	Forward primer to delete pre-miR-K3
	CGGGCGGTTCGTCGCTTGGACCTGGAGGGGTAGCCCATTACAGGCATTGTAGCTGTTGCG	Reverse primer to delete pre-miR-K3
	GATACCACGCAGCCGCGCATATTGGCGTTGTCACGGCCCGTGTGCCAGCCGCCTGGACG	Forward primer to delete pre-miR-K7
	CGTCCAGGCGGCTGGCACACGGGCCGTGACAACGCCAATATGCGCGGCTGCGTGGTATC	Reverse primer to delete pre-miR-K7
	CTATTCCAGTAGGTATACCCAGCTGGGTCTACCCGGCTGGGTAAATCCAGCTGTAATTC	Forward primer to delete pre-miR-K9
	GAATTACAGCTGGATTTACCCAGCCGGGTAGACCCAGCTGGGTATACCTACTGGAATAG	Reverse primer to delete pre-miR-K9
	TGCTGCCCAGGACGGCCGGATGCGGGCGTGAGGTAGTAGGTTGTATAGTTTTAGGG	Forward primer to insert pre-Let-7a-1
	CAGCGGATGTGTTTTGCCCAAACACGAGGAAAGACAGTAGATTGTATAGTTATCTC	Reverse primer to insert pre-Let-7a-1
Antisense LNAs	ATTGAATCAAACAGCCGACCAA	Control LNA
	GCTTACACCCAGTTTCCTGTAAT	LNA targeting miR-K1
	GGTTGCAGGAAACAGGTGCTGCC	LNA targeting miR-K1*
qPCR	CTTTGGTATCGTGGAAGGACT	*GAPDH* fw
	CCAGTGAGCTTCCCGTTCAG	*GAPDH* rev
	CCAGGGAAGCTGTTCGACTATTTC	*CYC1* fw
	CCAGGGAAGCTGTTCGACTATTTC	*CYC1* fw
	AAAACAGGAAGCGGGTTGGAC	*Pri-miR-K10/12* fw

	CCGCACCCTGCGTAAACAACC	*Pri-miR-K10/12* rev

T7 promoter sequence and LNA residues are underlined.

Table S2. Kinetic parameters for cleavage of KSHV miRNA hairpins within pri-miR-K10/12 by the Microprocessor *in vitro*.

	Exp#1			Exp#2		
pre-miR	***f* (%)**	**10 x k^+ (min^{-1})**	**100 x k^- (min^{-1})**	***f* (%)**	**10 x k^+ (min^{-1})**	**100 x k^- (min^{-1})**
K1	15.0 ± 1.0	1.50 ± 0.20	1.10 ± 0.20	17.0 ± 0.6	0.30 ± 0.01	3.00 ± 0.20
K2	1.7 ± 0.2	0.97 ± 0.20	0.32 ± 0.30	1.0 ± 0.1	0.53 ± 0.08	0.80 ± 0.30
K3	32.0 ± 2.0	0.82 ± 0.08	0.34 ± 0.20	40.0 ± 0.9	0.22 ± 0.005	2.20 ± 0.10
K4	15.0 ± 5.0	0.46 ± 0.20	1.70 ± 1.00	12.0 ± 12.0*	0.18 ± 0.18*	1.80 ± 1.80*
K5	11.0 ± 0.8	0.81 ± 0.09	0.57 ± 0.20	2.8 ± 0.6	0.58 ± 0.20	0.15 ± 0.50
K6	6.1 ± 5.0	0.38 ± 0.40	0.00 ± 2.00	2.8 ± 2.0	0.41 ± 0.30	0.00 ± 1.00
K11	11.0 ± 0.3	1.60 ± 0.10	1.10 ± 0.10	9.6 ± 9.6*	0.26 ± 0.26*	2.60 ± 2.60*
K7	3.4 ± 0.06	0.27 ± 0.005	2.70 ± 0.10	3.7 ± 0.1	0.14 ± 0.004	1.40 ± 0.10
K8	11.0 ± 0.5	2.30 ± 0.30	0.10 ± 0.10	13.0 ± 3.0	0.71 ± 0.20	1.80 ± 0.90
K9	7.0 ± 1.0	0.56 ± 0.10	0.05 ± 0.50	7.7 ± 6.0	0.32 ± 0.30	0.78 ± 2.00

Pre-miRNA accumulation levels *f* are in percentage of cleaved pri-miRNA in the assay (initial concentration = 16.7 nM, see Material and Methods). Cleavage rate constants k^+ and k^- are associated to cleavage by the Microprocessor or to residual Dicer or another RNase activity, respectively.

* when errors were extremely higher than the determined values, they were arbitrarily set at 100 %.

Table S3. Primary sequence and structural features determinants of miRNA stem-loops from KSHV pri-miR-K10/12.

Region or motif	Terminal loop	Basal stem		Flanking single-stranded segments	$U_{-14}G_{-13}$ from the 5' cleavage	GUG/UGU in apical loop	'mismatched GHG' at 7-9 nt from the basal junction	Shannon entropy along the miRNA stem	No of positive criteria
Criterion for optimal structure	([10-14] nt long)	~11 nt (±2)	Stable platforms	(at least one, ≥9 nt long)				low	
miRNA stem loop									
K3	Y (13)	Y (11)	Y	Y	Y	Y	N	Y	**7**
K1	Y (11)	Y (11)	Y	N	N	N	Y	Y	**5**
K11	Y (11)	Y (10)	Y	N	Y	Y	N	N	**5**
K8	Y (11)	N (7)	+/-	Y	N	Y	N	Y	**4.5**
K4alt	N (6)	Y (11)	Y	Y	N	N	N	Y	**4**
K6	N (9)	Y (11)	Y	Y	N	Y	N	N	**4**
K7	Y (14)	Y (13)	Y	N	N	Y	N	N	**4**
K9	N (8)	Y (11)	Y	N	N	N	N	Y	**3**
K4	N (6)	N (7)	+/-	N	N	N	N	Y	**1.5**
K2	N (16)	N (0)	N	N	Y	N	N	N	**1**
K5	N (9)	N (3)	+/-	N	N	N	N	N	**0.5**

H=any nt but G
In grey, expression is over 10%

SUPPLEMENTAL FIGURES AND LEGENDS

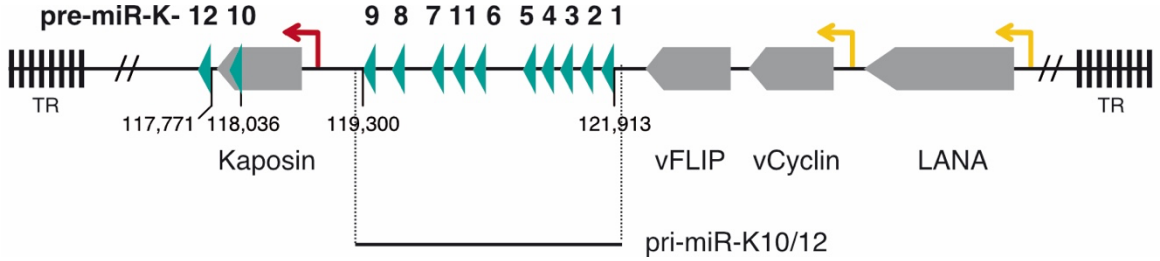

Figure S1. Genomic organization of KSHV miRNAs and location of pri-miR-K10/12. The twelve KSHV pre-miRNAs are localized in the latency locus and are indicated by green arrow heads. Ten of them are clustered in an intron (pre-miR-K1 to -K9 and pre-miR-K11) from which the sequence referred to as pri-miR-K10/12 derives, whereas pre-miR-K10 and -K12 are in the coding region and in the 3'UTR of Kaposin mRNA, respectively. Sequence coordinates were derived from reference sequence NC_009333.1. Open reading frames are in grey. Lytic promoter is represented by a red arrow and latent promoters by yellow arrows. TR, Terminal Repeats.

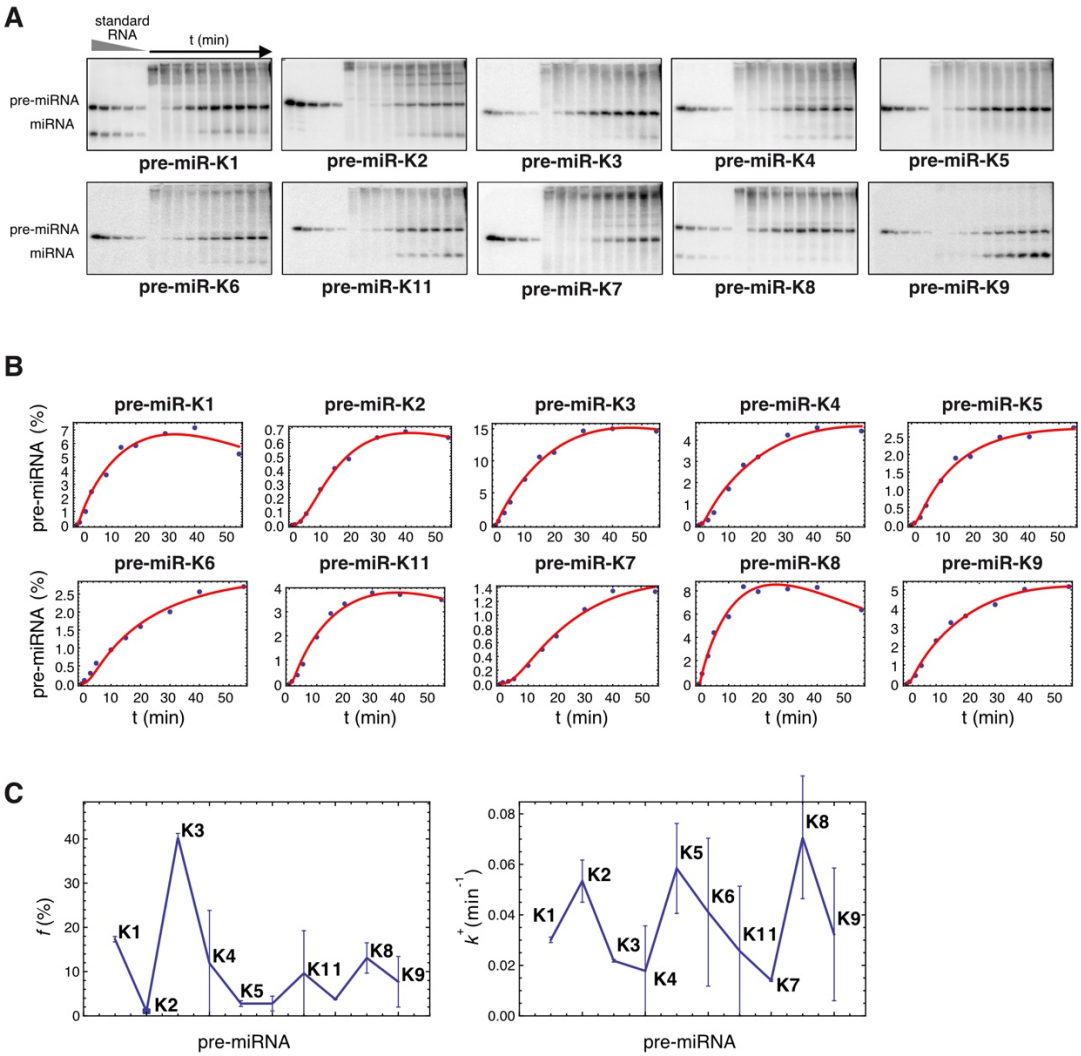

Figure S2. Kinetic analysis of KSHV clustered pre-miRNAs maturation *in vitro* by the Microprocessor (Exp#2).

(A) Northern blot analysis of the time course of *in vitro* processing assays using *in vitro* transcribed pri-miR-K10/12 and Hek293Grip cells total protein extract where Drosha and DGCR8 were overexpressed. *In vitro* transcribed pre-miRNAs and synthetic RNA oligonucleotides were loaded at decreasing concentrations as standards.

(B) Cleavage curves were obtained after plotting pre-miRNA product, in percentage of initial pri-miR-K10/12 substrate, according to time. The fits were obtained with the model involving three free parameters per curve (compare with Figure S3 for the more stringent model with two free parameters per curve).

(C) Processing efficiencies (left panel) and cleavage rate (right panel) were plotted in respect to miRNA hairpins showing variation among the clustered pre-miRNAs. The error bars come

from standard procedures used to fit the experimental curves by minimizing the residuals between the experimental points and their theoretical estimates.

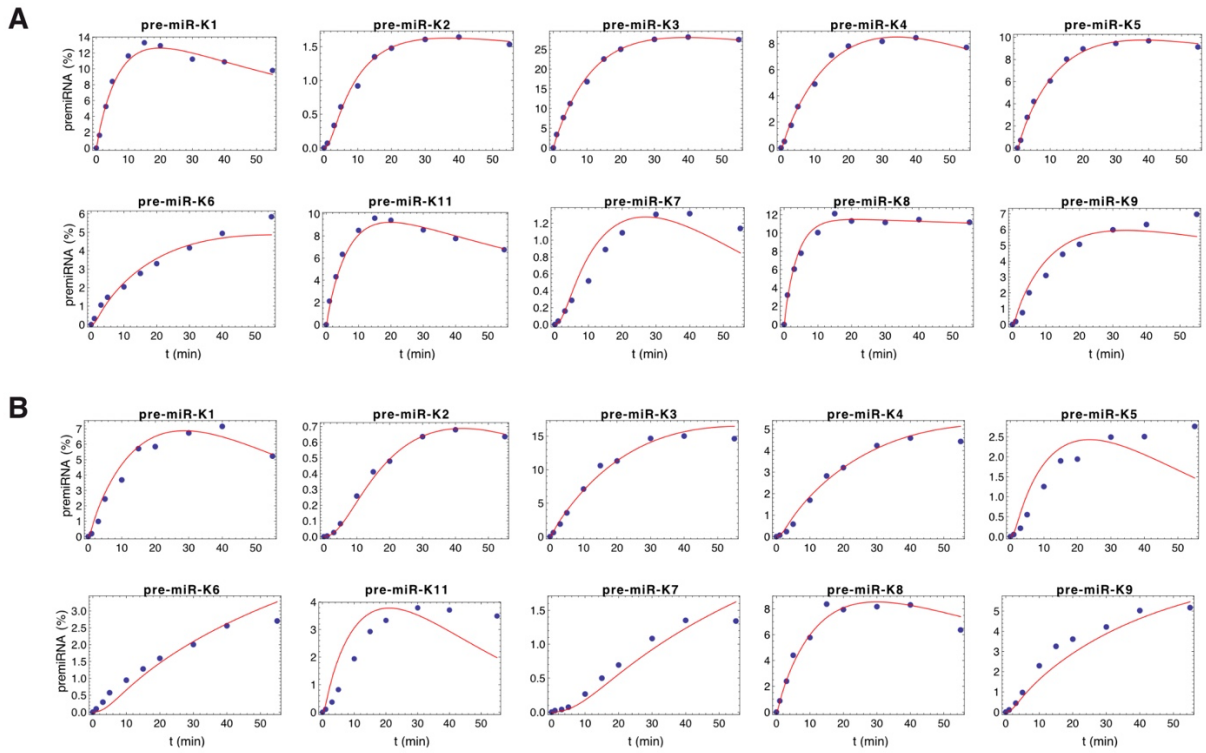

Figure S3. Joint fitting of the experimental curves for Exp#1 (A) and Exp#2 (B) with two free parameters per curve.

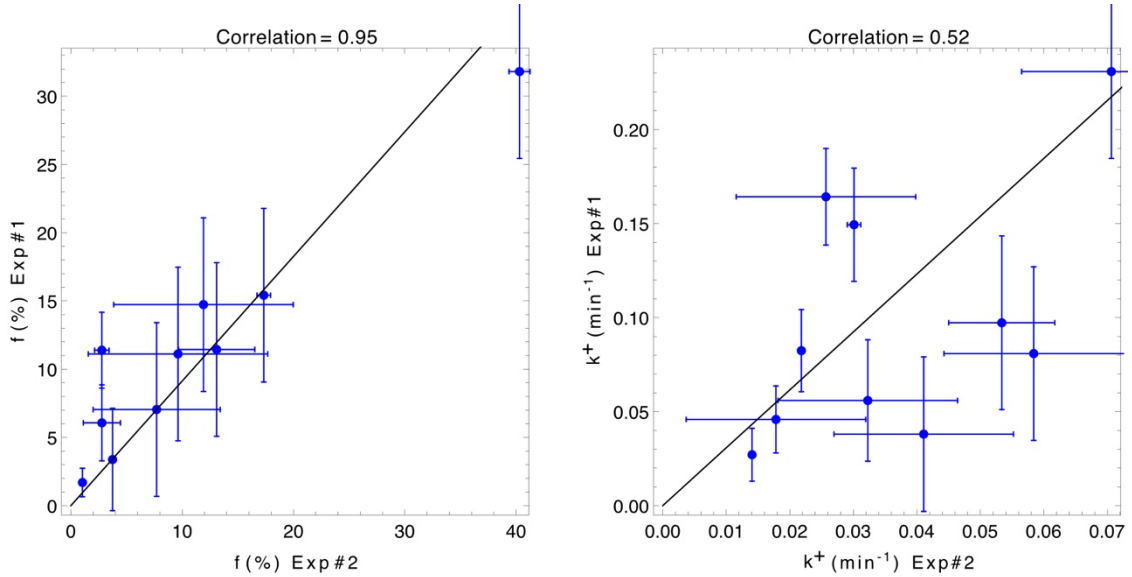

Figure S4. Correlation among experiments of *in vitro* processing assays.
Processing efficiencies (*f* in percentage, left panel) and cleavage rate constants (k^+ in min^{-1}, right panel) were compared between the two experiments analyzed in this study, namely Exp#1 and Exp#2.

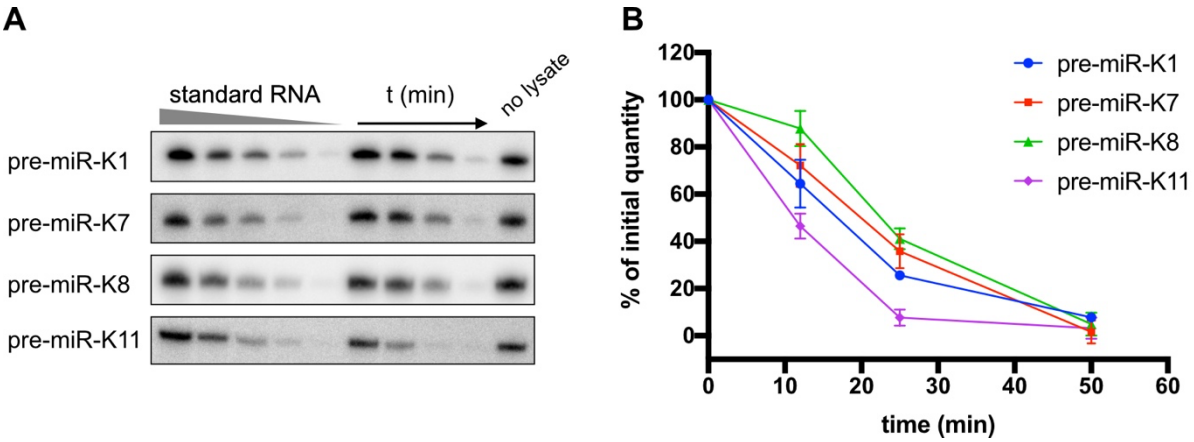

Figure S5. Determination of synthetic pre-miRNAs stability in processing assays.

In vitro transcribed pre-miRNAs were incubated in whole cell lysate from HEK293Grip cells and submitted to conditions used for *in vitro* processing assays. Their decay was followed over time. Northern blots (A) were quantified by using standard pre-miRNAs and results from three replicates were plotted (B) relative to pre-miRNA quantity at 0 min.

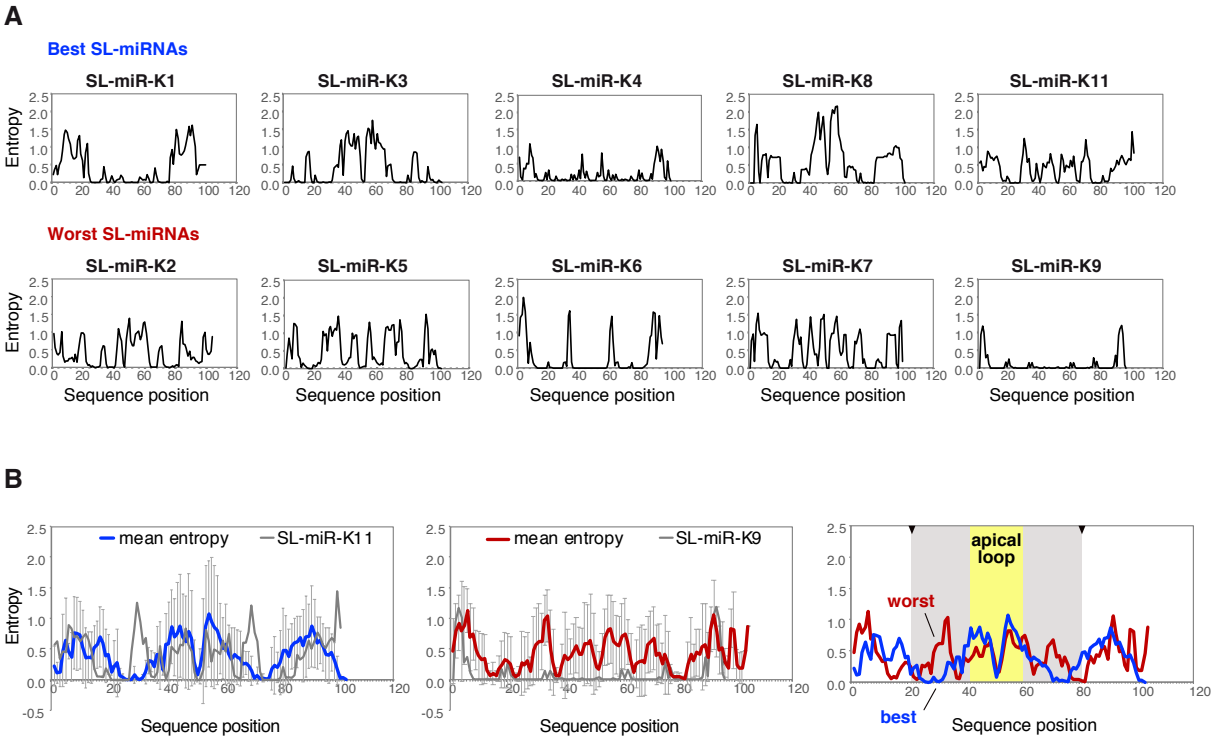

Figure S6. Positional entropy of KSHV miRNA hairpins.

(A) Shannon entropy was plotted across the sequence of individual miRNA hairpins, namely stem-loop (SL)-miRNAs, including the pre-miRNA plus 20 nucleotides on both sides, using RNAfold from ViennaRNA Web Services (Institute for Theoretical Chemistry, University of Vienna) (1, 2).

(B) Mean entropies of the best substrates (processed over 10%, blue curve, left panel) and of the worst substrates (processed below 10%, red curve, middle panel) were plotted across the sequence. Comparison of the two curves (right panel) show that the best substrates are enriched for low entropy along the stem in contrast to the worst substrates, in agreement with data published in Rice et al (3). However, in the two groups, exceptions come with SL-miR-K11 (processed over 10% but showing high entropy along the stem, grey curve, left panel) and SL-miR-K9 (processed below 10% but showing low entropy, grey curve, middle panel). The approximate location of apical loop and the stem is highlighted in yellow and grey, respectively, and cleavage sites are indicated by arrow heads.

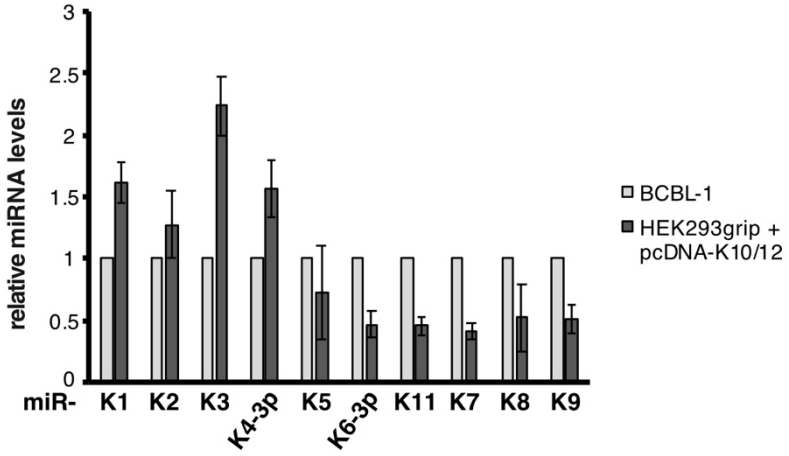

Figure S7. Relative expression of KSHV miRNAs from HEK293grip cells transiently transfected with pcDNA-K10/12 compared to expression in BCBL-1 infected cells. Values were obtained by quantifying signals from northern blot analysis. Error bars derive from three independent experiments except for miR-K1, -K2, -K4-3p and -K6-3p where n=2.

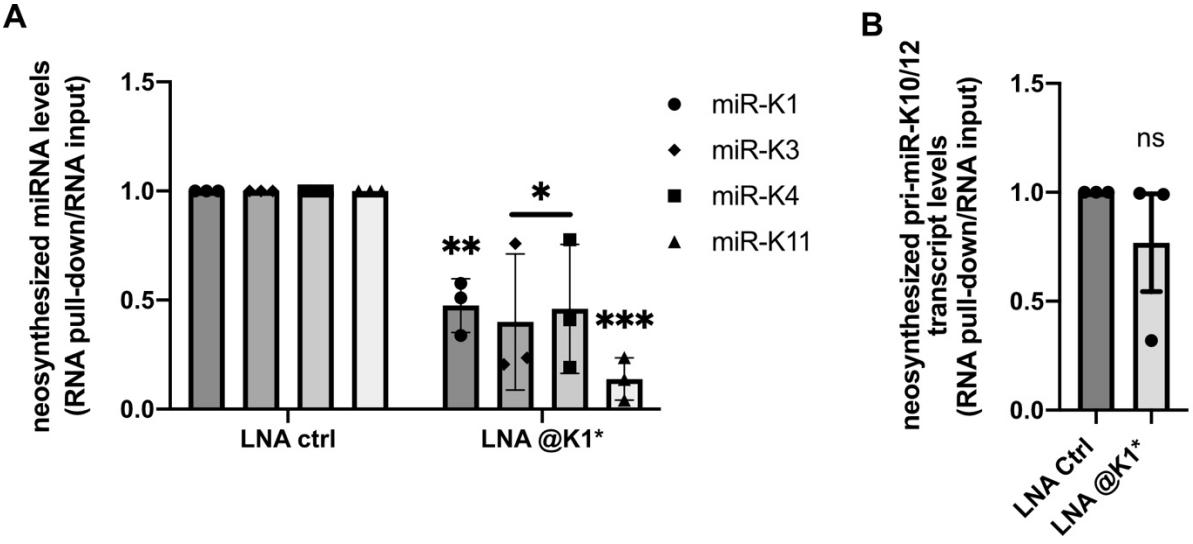

Figure S8. Quantification of neosynthesized miRNAs upon treatment with 20 nM of LNA oligonucleotides.

HEK293FT-rKSHV cells were transfected with 20 nM LNA complementary to miR-K1* or control LNA. 24 hours after transfection, they were incubated with 100µM 4sU for another 16 hours. Neosynthesized transcripts having incorporated 4sU were isolated and levels of mature miRNAs (A) and primary transcript (B) were measured by RT-qPCR. Histograms show ratios of enrichment in pull-down over input RNA relative to Let-7 levels which were set to 1 in control samples. Enrichment of primary transcript was determined relative to CYC1. Bars represent mean ± s.e.m of three experiments. Statistical significance was verified by unpaired t test with ns: non-significant, *: $p < 0.05$, **: $p < 0.01$, ***: $p < 0.001$.

Supplemental bibliography

1. Gruber,A.R., Lorenz,R., Bernhart,S.H., Neubock,R. and Hofacker,I.L. (2008) The Vienna RNA Websuite. *Nucleic Acids Res.*, **36**, W70–W74.
2. Lorenz,R., Bernhart,S.H., Höner zu Siederdissen,C., Tafer,H., Flamm,C., Stadler,P.F. and Hofacker,I.L. (2011) ViennaRNA Package 2.0. *Algorithms Mol. Biol.*, **6**.
3. Rice,G.M., Shivashankar,V., Ma,E.J., Baryza,J.L. and Nutiu,R. (2020) Functional Atlas of Primary miRNA Maturation by the Microprocessor. *Mol. Cell*, **80**, 892-902.e4.